Electrochemical sensing of NADH based on Meldola Blue immobilized silver nanoparticle-conducting polymer electrode

A. Balamurugan [a,b,1], Kun-Cheng Ho [b], Shen-Ming Chen [b,*], Tzu-Yen Huang [b]

[a] Graduate Institute of Engineering Technology, National Taipei University of Technology, No. 1, Section 3, Chung-Hsiao East Road, Taipei 106, Taiwan, ROC
[b] Department of Chemical Engineering and Biotechnology, National Taipei University of Technology, No. 1, Section 3, Chung-Hsiao East Road, Taipei 106, Taiwan, ROC

ARTICLE INFO

ABSTRACT

Silver nanoparticles (nanoAg) incorporated poly(3,4-ethylene dioxythiophene-sodium dodecyl sulfate) (PEDOT$_{SDS}$) modified electrode was prepared by electrochemical deposition method. Hereafter, the above-modified electrode denoted as PEDOT$_{SDS}$–nanoAg electrode. The nanoAg formation was confirmed by UV–vis spectroscopy and it shows surface plasmon resonance (SPR) peak at 375 nm. The surface morphology, film thickness, and surface roughness of PEDOT$_{SDS}$–nanoAg electrode were studied using atomic force microscopy (AFM). The PEDOT$_{SDS}$–nanoAg electrode has been utilized as a platform to immobilize electrochemically active mediator, Meldola Blue (MDB), by means of electrostatic trapping and the electrode denoted as PEDOT$_{SDS}$–nanoAg–MDB electrode. At 750 s of silver deposition time, reversible redox peak of MDB, which existed on PEDOT$_{SDS}$–nanoAg–MDB electrode, was obtained and that time was found to be an optimum. The electrochemical properties of the PEDOT$_{SDS}$–nanoAg–MDB electrode were studied by cyclic voltammetry (CV). The PEDOT$_{SDS}$–nanoAg–MDB electrode was investigated for catalytic application, which shows electrocatalytic activity towards the oxidation of NADH (dihydronicotinamide adenine dinucleotide) with 650 mV decrease in overpotential in comparison with bare glassy carbon electrode. Using the PEDOT$_{SDS}$–nanoAg–MDB electrode, the amperometric measurements were performed at an applied potential of −0.05 V and a linear response of NADH was obtained in the range from 10 to 560 μM with a limit of detection (LOD) of 0.1 μM. The PEDOT$_{SDS}$–nanoAg–MDB electrode showed diminished response to its interferences.

© 2010 Elsevier B.V. All rights reserved.

1. Introduction

The electrochemical oxidation of NADH to NAD$^+$ provides an attractive model system on which to test ideas about the design of modified electrodes [1]. The oxidation of NADH to NAD$^+$ involves the transfer of two electrons and one proton and cleavage of C–H bond. Direct electrochemical oxidation of NADH to NAD$^+$ at the bare electrode surface is highly irreversible and takes place at high overpotential (large activation energy) and is accompanied by rapid poisoning of the reaction because the electrode surface is fouled by the polymeric products of the side reactions [2,3], which occur because the one electron oxidation intermediates formed in the reaction are unstable and highly reactive. Various methodologies have been developed to facilitate the electron transfer kinetics [4].

A convenient way to decrease the high overpotential and avoid the surface fouling is to use of redox mediators that can promote the

electron transfer kinetics. In this way, much effort has been devoted to identify/develop new materials which can effectively overcome the kinetic barriers for the electrochemical regeneration of enzymatically active NAD$^+$ [5,6]. The phenazines [7], phenothiazines [8], nitrofluorenone [5], oxidation product of NAD$^+$ [9], quinone [10] and their derivatives have been either adsorbed, electropolymerized or covalently attached to the electrode surface and utilized for the electrocatalytic oxidation of NADH. Besides, the mediators are also immobilized in different kind platforms to fabricate the NADH sensing electrode in order to improve stability, selectivity and sensitivity of the electrode. Such a kind platforms are, e.g. metal oxide [11], carbon nanotubes (CNTs) [12,13], sol–gel [14], Nafion [15], and nucleic acids (DNA) [16]. Though, such platforms offer an increased performance of the modified electrode for NADH sensing, however, there are disadvantages still occurring. Such disadvantages are (i) Nafion is an anionic polymer will hinder the approach of NADH [13], and (ii) leaching of mediators are easy in the case of sol–gel technique, and (iii) in many cases, the decrease of the overpotential is not sufficiently low to eliminate its interferences from other easily oxidizable species in real samples [17].

In recent times, the fabrication of nanomaterial-based electrodes has been received great attention since it has larger surface

---

area and quantum size effect, etc. In this way, much effort has been devoted to identifying/developing new materials which can effectively overcome the kinetic barriers for the oxidation of NADH and regenerate the enzymatically active NAD^{+} [6,18]. Palladium [19] and gold nanoparticles [6] modified electrodes can effectively catalyze oxidation of NADH. Also, CNTs based electrodes have been shown to decrease the overpotential for the oxidation of NADH [12,13]. Moreover, conducting polymer [20] and conducting polymer–metal nanocomposites have been fascinated field of research for NADH oxidation. Recently, Tian et al. [21,22] have been studied electrochemical properties of polyaniline-gold nanocomposite film electrode and showed excellent redox activity as well as film can electrocatalytically oxidizes NADH. Since, conducting polymers have been proven to be suitable host matrices for dispersing metallic particles. Furthermore, the composites of conducting polymers with metal nanoparticles permit a facile flow of electronic charges across the polymer matrix during electrochemical processes [23]. More recently, Manesh et al. [24] have employed the gold nanoparticles loaded PEDOT–PSS modified electrode for electrocatalytic oxidation of NADH. The use of poly (sodium 4-styrene sulfonate) (PSS) enhances the solubility of EDOT in an aqueous media since the solubility of EDOT itself in aqueous media is not adequate enough to form film [25]. Considering the unique properties of conducting polymer–metal nanoparticle composite, we interested to immobilize positively charged MDB on the negatively charged PEDOT$_{SDS}$–nanoAg electrode.

In the present investigation, first, we prepared SDS incorporated PEDOT–nanoAg electrode by electrochemical deposition method, denoted as PEDOT$_{SDS}$–nanoAg electrode. The use of surfactant (SDS), as an alternate for PSS, increases the solubility of EDOT in an aqueous media by forming pseudo-complex and the backbone of PEDOT is incorporated by negatively charged sulfonate moieties of SDS [26]. Secondly, by taking advantage of negatively charged PEDOT$_{SDS}$–nanoAg electrode, we have applied to immobilize positively charged MDB. Finally, the utility of PEDOT$_{SDS}$–nanoAg–MDB electrode has been examined for electrocatalytic oxidation of NADH. In addition, the presence of nanoAg on PEDOT$_{SDS}$–nanoAg–MDB electrode also enhanced the reversibility of redox peak of MDB by acting as an "*electron relay*" [27]. To our knowledge, this is the first report for use of PEDOT$_{SDS}$–nanoAg electrode as a platform to immobilize an electrochemically active mediator, MDB.

2. Materials and methods

2.1. Reagents and solutions

EDOT, Meldola Blue, dopamine (DA), uric acid (UA), ascorbic acid (AA), and NADH were purchased from (Sigma–Aldrich). Silver nitrate and hydrogen peroxide (H_2O_2) (33%) were obtained from Wako Chemicals. All reagents were of analytical grade and used without any further purification. Solutions were prepared with doubly distilled water. High purity nitrogen was used for deaeration. The buffer and sample solutions were purged with highly purified nitrogen for at least 20 min prior to the experiments. Nitrogen atmosphere was maintained over the solutions during experiments.

2.2. Apparatus

Electrochemical experiments were performed with CH Instruments (Model CHI-400) using CHI-750 potentiostat. Glassy carbon electrode (geometric area = 0.07 cm^2) obtained from Bioanalytical Systems (BAS) served as a working electrode and Pt wire act as counter electrode. All the potentials given in this paper were referred with respect to Ag/AgCl (saturated KCl solution) reference electrode. Indium tin oxide coated glass electrode (ITO electrode) was used to obtain Atomic force microscope (AFM) images. AFM images were recorded by Beijing Nano-Instruments CSPM4000 using tapping mode operation. Rectangle Si$_3$N$_4$ cantilevers with a normal force constant, 0.4 N/m, a radius of less than 10 nm were employed. Ultraviolet–visible (UV–vis) spectra were recorded on a model U-3300 UV–vis spectrophotometer (Hitachi).

2.3. Preparation of different types of PEDOT–MDB modified electrode

Prior to modification, glassy carbon electrode (GCE) was polished with 0.05 μm alumina on Buehler felt pads and then ultrasonically cleaned for about a minute in water. Finally, the electrode was washed thoroughly with double distilled water and used. After being cleaned, the polished GC surface was subjected to electrochemical deposition to prepare different types of PEDOT–MDB modified electrode. The PEDOT modified electrode was prepared potentiodynamically (for three potential cycles) by scanning the electrode from −0.6 to 1.0 V in aqueous solutions containing 0.01 M EDOT, 0.10 M LiClO$_4$ in the presence (denoted as, PEDOT$_{SDS}$ electrode) and absence (denoted as, PEDOT electrode) of 0.050 M SDS, respectively. Then, PEDOT–Ag and PEDOT$_{SDS}$–nanoAg electrode were prepared by potentiostatic method. Typically, PEDOT and PEDOT$_{SDS}$ electrodes were immersed in 0.1 M NaNO$_3$ solutions containing 1 mM AgNO$_3$ and electrodeposited at −0.4 V for 750 s. Finally, PEDOT–Ag, PEDOT$_{SDS}$, and PEDOT$_{SDS}$–nanoAg electrodes were separately dipped in 0.5 mM MDB solution for about 10 min. The schematic representation of PEDOT$_{SDS}$–nanoAg–MDB electrode is shown in Scheme 1. The above three modified electrodes were thoroughly washed further with extra pure water to
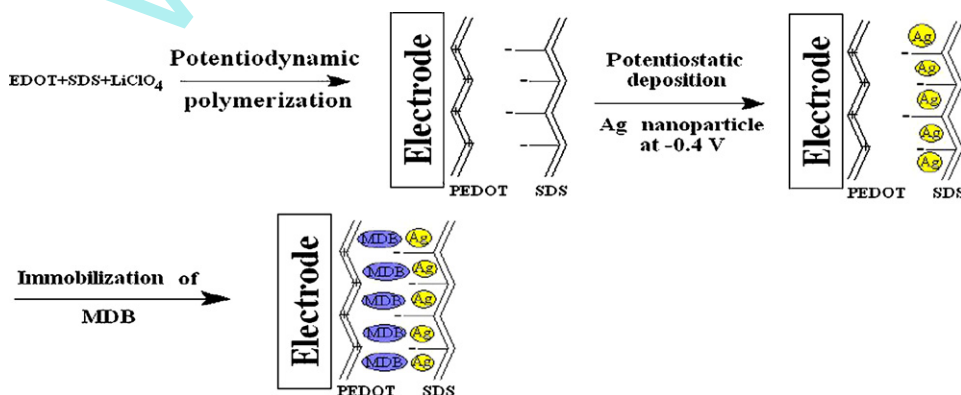
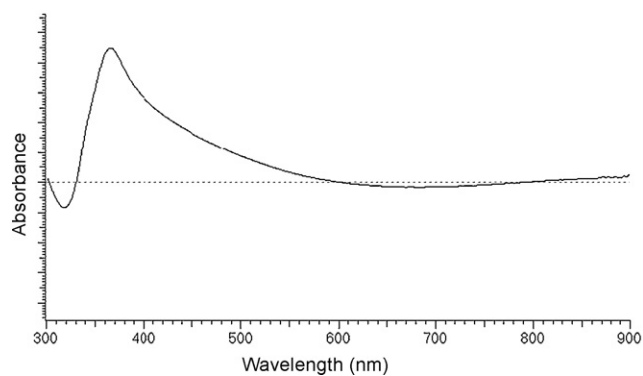**Scheme 1.** Preparation steps of PEDOT$_{SDS}$–nanoAg–MDB electrode.

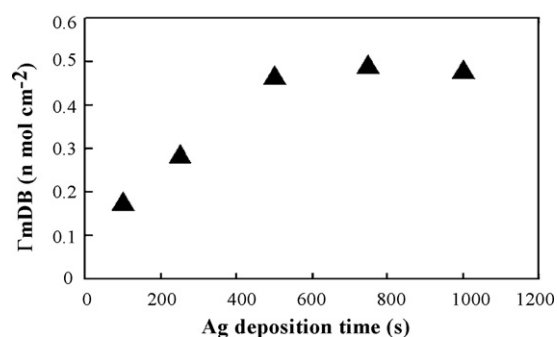**Fig. 1.** UV–vis spectrum of PEDOT$_{SDS}$–nanoAg ITO electrode.

Fig. 3. The plot of silver deposition time vs surface coverage of MDB on PEDOT$_{SDS}$–nanoAg–MDB electrode. Electrolyte: PBS solution, pH 7 and scan rate: 50 mV/s.

remove unadsorbed MDB and stored in the phosphate buffer for further studies.

3. Results and discussion

3.1. Characterization of PEDOT$_{SDS}$–nanoAg electrode using UV–vis spectroscopy and Atomic force microscopy

The PEDOT$_{SDS}$–nanoAg electrode visibly exhibits yellowish transparent film, which is an indication for the formation of nanoAg. In addition, PEDOT$_{SDS}$–nanoAg modified ITO electrode was monitored by UV–vis spectroscopy in the region 200–900 nm, which shows absorption peak at 375 nm, as shown in Fig. 1. This absorption peak corresponds to SPR peak of nanoAg [28], indicating the formation of silver nanoparticles on PEDOT$_{SDS}$ electrode.

Surface morphologies of PEDOT$_{SDS}$ and PEDOT$_{SDS}$–nanoAg electrode were analyzed by atomic force microscopy (AFM), as shown in Fig. 2. PEDOT$_{SDS}$–nanoAg electrode (Fig. 2A) appeared smooth and the arrangement of nanoAg was highly order as well as appeared as small discrete chain like structure. It might be due to the presence of negatively charged SDS on PEDOT$_{SDS}$ electrode, which restricts the mobility of nanoAg from an agglomeration and also assist for stabilization of nanoparticles. The thickness of modified electrode was measured using AFM cross-sectional analysis and found to be 230 nm. The average particle size of silver was ≈120 nm. Moreover, surface roughness of PEDOT$_{SDS}$–nanoAg electrode was measured

using 2D AFM and was found 32.2 nm. Fig. 2B shows the AFM image of PEDOT$_{SDS}$ modified electrode and it appeared as globules with rough surface, which is in agreement with our earlier report [29] and its surface roughness, height were 9.7 nm and 95 nm, respectively.

3.2. Optimization of silver nanoparticles deposition in PEDOT$_{SDS}$ modified electrode

To obtain a much larger effective surface area of electrode and provide a good environment for MDB immobilization, silver deposition time was optimized by scanning the MDB immobilized PEDOT$_{SDS}$–nanoAg electrode in PBS solution. Fig. 3 shows the relationship between the surface coverage of anodic peak current of MDB on PEDOT$_{SDS}$–nanoAg–MDB electrode and silver electro deposition time. From Fig. 3, it can be noticed that surface coverage of PEDOT$_{SDS}$–nanoAg–MDB electrode increased as deposition time increased from 100 to 750 s. When the deposition time was 750 s, the surface coverage of electrode reached the maximum value and also reversibility, i.e., Ip_a/Ip_c also unity. When the deposition time exceeded 750 s, the surface coverage of electrode decreased slightly. Hence, 750 s of silver deposition time was selected as an optimum in order to obtain reversible redox peak of MDB.
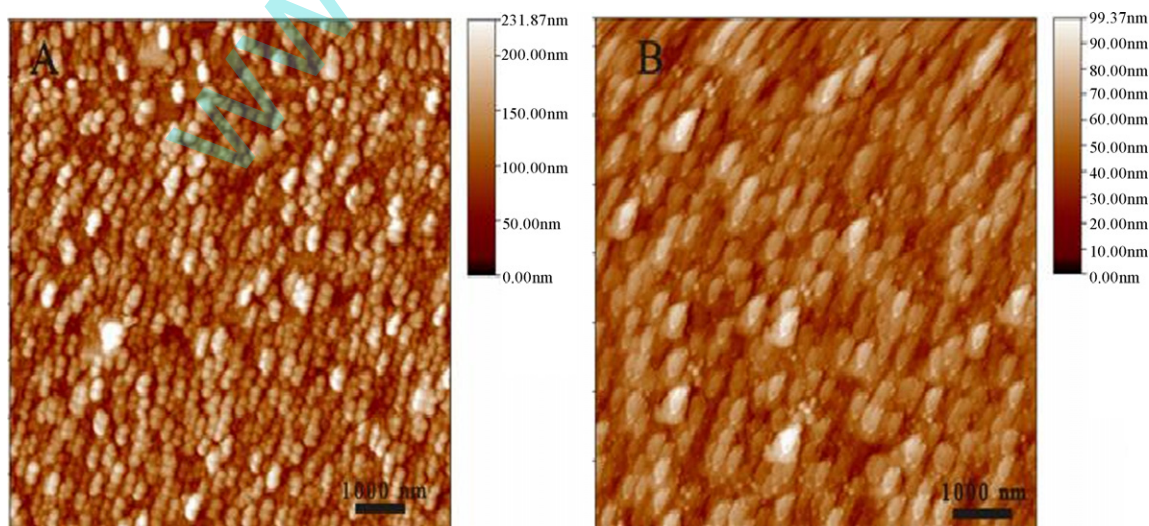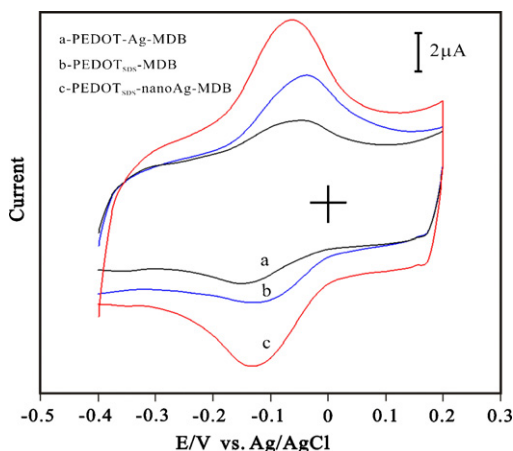

Fig. 2. AFM images of (A) PEDOT$_{SDS}$–nanoAg electrode, and (B) PEDOT$_{SDS}$ electrode.

Fig. 4. CV response of (a) PEDOT–Ag–MDB, (b) PEDOT$_{SDS}$–MDB, and (c) PEDOT$_{SDS}$–nanoAg–MDB electrodes. Electrolyte; PBS solution, pH 7 and scan rate: 50 mV/s.

3.3. Electrochemical study of PEDOT$_{SDS}$–nanoAg–MDB electrode

Fig. 4 shows CVs of different MDB–PEDOT modified electrode in pH 7 phosphate buffer solutions (PBS). As shown in Fig. 4a, PEDOT–Ag–MDB electrode magnitude of peak current was small and ΔE_p was 100 mV. It indicates that electron transfer was sluggish and adsorption of MDB on the electrode had not strong. On the other hand, magnitude of peak current of MDB on PEDOT$_{SDS}$–MDB (Fig. 4b) and PEDOT$_{SDS}$–nanoAg–MDB electrodes (Fig. 4c) were higher than PEDOT–Ag–MDB. ΔE_p was 80 and 65 mV for PEDOT$_{SDS}$–MDB electrode and PEDOT$_{SDS}$–nanoAg–MDB electrode, respectively. Thus, the SDS incorporated electrodes were exhibited higher magnitude of peak current and lower ΔE_p than an electrode without SDS (PEDOT–Ag–MDB), which might be due to electrostatic interaction between negatively charged SDS which is incorporated in PEDOT [26] and a positively charged MDB dye [30].

Now, it is worth to compare the magnitude of peak current and reversibility between PEDOT$_{SDS}$–MDB and PEDOT$_{SDS}$–nanoAg–MDB electrode. The higher magnitude of peak current and reversibility ($Ip_a/Ip_c = 1$ and $\Delta E_p = 65$ mV) at PEDOT$_{SDS}$–nanoAg–MDB electrode was observed than PEDOT$_{SDS}$–MDB electrode ($Ip_a/Ip_c \neq 1$ and $\Delta E_p = 85$ mV). The observed significant increase in the magnitude of peak current and reversibility at PEDOT$_{SDS}$–nanoAg–MDB electrode, which might

due to the presence of nanoAg in the electrode. It is well known that metal nanoparticles provide good platform for increasing electrochemical signal due to high surface area as well as the presence of free electrons [31,32]. The presence of stabilized nanoAg at the PEDOT$_{SDS}$–nanoAg–MDB electrode supplies excess of free electrons and it acts as an "*electron relay*" between MDB and PEDOT$_{SDS}$, thereby, facilitates redox peak of MDB with high reversibility, as shown in Fig. 4c. The stabilization of nanoAg achieved through an interaction between negatively charged SDS which is incorporated in the PEDOT, as shown in Scheme 1. Similar type of results was observed by Ramasubbu et al. [27] at the composite of thionine immobilized silver/clay modified electrode. They were observed higher magnitude of peak current with reversible redox peak of thionine at thionine immobilized silver/clay modified electrode than thionine immobilized/clay modified electrode. Finally, they ascribed reason, for higher magnitude of peak current, and reversibility, which might be due to the presence of silver nanoparticles that act as an electron relay between thionine dye and clay electrode. In this context, it is also relevant to mention a similar observation reported by Jana et al. [33]. In this case of SDS stabilized silver nanoparticles have higher catalytic activity than silver nanoparticles for the reduction of positively charged dye.

It is also worth to compare the electrochemical behavior of MDB on PEDOT$_{SDS}$–nanoAg–MDB electrode with other electrodes based on calcium, titanium and zirconium phosphates, niobium oxide, etc. [34,35]. The calcium, titanium and niobium oxide ($E^{0\prime}$ at −60 mV at pH 7 vs Ag/AgCl) based electrodes show the redox peak for MDB at more positive potentials [34,35] than that is observed in the present PEDOT$_{SDS}$–nanoAg–MDB electrode ($E^{0\prime}$ −100 mV); the ΔE_p value at these electrodes [34,35] is relatively larger as well as ratio of Ip_a/Ipc is not unity. These results imply that nanoAg on PEDOT$_{SDS}$–nanoAg–MDB electrode plays vital role to enhance the electrochemical properties.

3.4. Electrochemical characterization of PEDOT$_{SDS}$–nanoAg–MDB electrode

The electrochemistry of the PEDOT$_{SDS}$–nanoAg–MDB electrode was studied by CV at various scan rates. Fig. 5A shows the CVs of PEDOT$_{SDS}$–nanoAg–MDB electrode in pH 7 PBS solution and highly reversible peak was observed with formal potential of redox couple ($E^{0\prime}$), at −0.1 V and both anodic and cathodic currents increase linearly with scan rates up to 0.2 V s^{-1} as shown in Fig. 5. Also, the ratio of anodic to cathodic peak currents was unity for all scan rates studied. All of these features are consistent with those anticipated
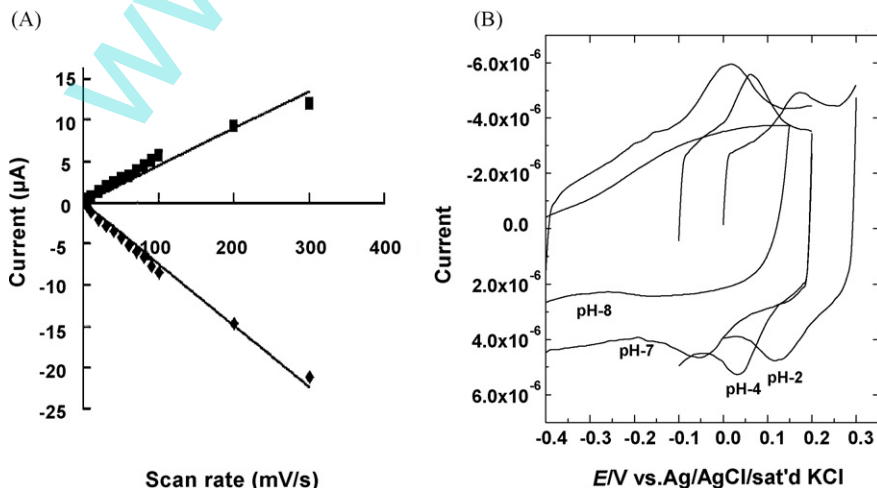
Fig. 5. (A) The plot of current vs scan rate of PEDOT$_{SDS}$–nanoAg–MDB electrode. (B) pH study of PEDOT$_{SDS}$–nanoAg–MDB over pH range 2–8. Scan rate 0.05 V/s.

for a reaction involving surface-confined species and the charge transfer is fast in the coating [36].

We have estimated, the apparent surface coverage, Γ by using the following equation:

$$\Gamma = \frac{Q_t}{nFA_e}$$

where Q_t is charge from the area under the PEDOT$_{SDS}$–nanoAg–MDB electrode oxidation peak corrected for the base line (at the scan rate of $10\,\text{mV}\,\text{s}^{-1}$); A_e is the surface area ($0.07\,\text{cm}^2$) and the other symbols have their usual meanings. In the present case, the calculated surface coverage (Γ) is $5.56 \times 10^{-10}\,\text{mol}\,\text{cm}^{-2}$ for $n = 2$. This value is comparable with other MDB modified electrodes such as CNT/Chit-MDB modified electrode ($6.23 \times 10^{-10}\,\text{mol}\,\text{cm}^{-2}$) [13], Zirconium phosphate/MDB modified electrode ($9.9 \times 10^{-10}\,\text{mol}\,\text{cm}^{-2}$) [37], and four times larger than that of MDB/CNTs/GC electrode ($1.8 \times 10^{-10}\,\text{mol}\,\text{cm}^{-2}$) [38], and two times larger than electropolymerized MDB electrode ($3.61 \times 10^{-10}\,\text{mol}\,\text{cm}^{-2}$) [39].

Fig. 5B displays the pH-dependent cyclic voltammetric response of PEDOT$_{SDS}$–nanoAg–MDB electrode. In order to ascertain this, cyclic voltammetric responses of PEDOT$_{SDS}$–nanoAg–MDB electrode were obtained in different pH solutions. As increase the pH of contact solution, formal potential of the electrode shift towards negative potential. The redox peak current of the electrode is almost same up to pH 7. But at the higher pHs (above the pH 7) redox peak current is decreased. Plot of formal potential vs pH yields the slope of $-59\,\text{mV/pH}$ for the pH up to 7. This suggests that equal number of protons and electrons takes part in electrochemical reaction. Similar behavior was noticed by Zhu et al. for MDB over modified electrode [38].

3.5. Electrocatalytic oxidation of NADH at PEDOT$_{SDS}$–nanoAg–MDB electrode

One of the objectives of the present study is to fabricate modified electrode that is capable for the electrocatalytic oxidation of NADH. It is well known that p-quinone-imines which derived from dye and adenine derivatives [9,40] are catalytically active for the oxidation of NADH. In order to examine the electrocatalytic activity of the PEDOT$_{SDS}$–nanoAg–MDB electrode, the CVs were recorded with and without NADH and results are shown in Fig. 6. When an addition of NADH there was a marked enhancement of the anodic peak current at potentials close to anodic peak potential about $-0.05\,\text{V}$ along with a concomitant decrease of the cathodic peak current was observed at the modified elec-
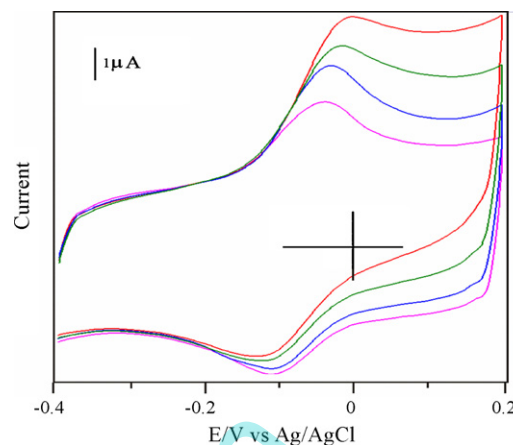

Fig. 6. CVs of different concentrations of NADH at PEDOT$_{SDS}$–nanoAg–MDB electrode. Concentrations of NADH (inner to outer) are 0, 0.1, 0.3, 0.5 mM. Scan rate: 50 mV/s and electrolyte: PBS solution, pH 7.

trode. The enhancement of anodic peak current in the presence of NADH comes from mediated oxidation of NADH to NAD$^+$, i.e., NADH reduces the oxidized mediator (PEDOT$_{SDS}$–nanoAg–MDB$_{ox}$) to form NAD$^+$ and reduced form mediator (PEDOT$_{SDS}$–nanoAg–MDB$_{red}$) which in turn is electrochemically regenerated, as shown in the Eq. (1). At the bare glassy carbon electrode oxidation of NADH occurs at around 0.6 V (vs Ag/AgCl). The oxidation peak current increases linearly with increasing the square root of scan rate, suggesting oxidation process is diffusion controlled. The marked enhancement in the anodic peak current and a decrease in over potential about 650 mV were observed at PEDOT$_{SDS}$–nanoAg–MDB electrode, which demonstrates the strong electro catalytic effect of the PEDOT$_{SDS}$–nanoAg–MDB electrode. Upon the addition of NADH, an increase in the anodic peak current was observed in the forward scan and a concomitant decrease in the cathodic peak current was noticed in the reverse scan. However, the decrease in the cathodic peak current was not as appreciable as that found in the anodic side. Probably, it might be due to diffusion of NADH to the electrode surface. Similar observation was made by Rosca et al. at phenothiazine derivative modified electrode for electrocatalytic oxidation of NADH [41]. Catalysis is then a result of the diffusion of NADH to the electrode surface, where it reduces MDB$_{ox}$ to form NAD$^+$ and MDB$_{red}$,

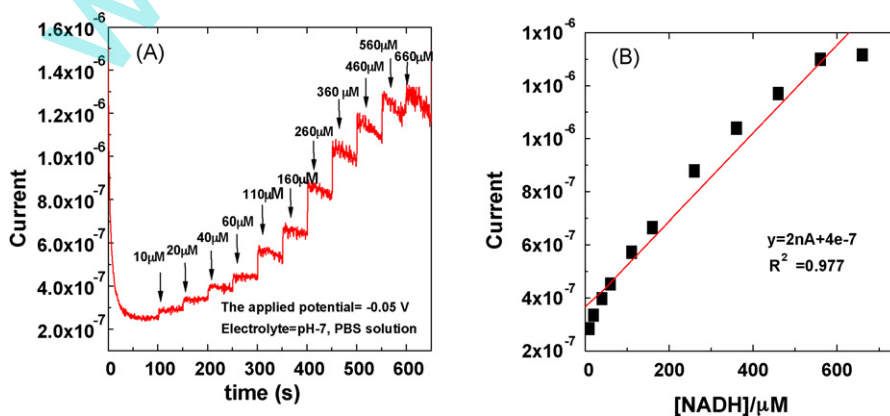$$MDB_{ox} + NADH \rightarrow MDB_{red} + NAD^+ \tag{1}$$

Fig. 7. (A) Amperometric response of NADH at PEDOT$_{SDS}$–nanoAg–MDB electrode under stirring condition. Electrolyte: PBS solution, pH 7, and operating potential = $-0.05\,\text{V}$. (B) Calibration curve. Noise might be due to stirring of an electrolyte.

Table 1
Comparison of detection limit, and working potential of present PEDOT$_{SDS}$–nanoAg–MDB electrode with other references.

Modified electrodes	Working potential	Linear range	Detection limit	Sensitivity	Ref.
Highly boron-doped electrode	0.6 vs SCE	10–500 nM	10 nM	–	[42]
PEDOT–PSS–AuNPs electrode	0.04 vs Ag/AgCl	0.1–2.2 μM	–	88 ± 2 mA/M cm^2	[24]
Edge plane pyrolytic graphite electrode	+0.4 V Ag/AgCl	–	3.3×10^{-7} M	–	[43]
MDB/CNT–chitosan electrode	−0.14 V vs Ag/AgCl	Up to 80 μM	0.5 μM.	5.9 ± 1.52 nA/μM)	[13]
MDB/SiO$_2$/TiO$_2$/graphite electrode	−0.12 V vs SCE	0.018 to 7.29 mM	8 μM	–	[30]
MDB/CNT/GC electrode	−0.1 V vs Ag/AgCl	Up to about 500 μM	0.048 μM	0.52 ± 0.02 μA/mM	[38]
AuNPs electrode	+0.39 V vs SCE (pH 2.4)	$7.5 \times 10^{-7} - 2.5 \times 10^{-6}$	2.5×10^{-7} M	–	[44]
o-Aminophenol modified electrode	0.15 V (vs Ag/AgCl	$7.5 \times 10^{-7} - 2.5$ μM	1.5×10^{-7} M	–	[45]
FCNT/Chit composite electrode	−0.03 V Ag/AgCl	–	0.1 μM	134.3 ± 1 nA cm^{-2} μM	[46]
Nile Blue (NB)/(OMC) electrode	−0.1 V.	Up to 350 μM	1.2 μM	648 nA/mM	[47]
Graphite/poly(methylmethacrylate) electrode	−0.35 V vs Ag/AgCl	4.0 μM to 5.6 mM	3.5 μM	68 mA M^{-1} cm^{-2}	[48]
Au/PANI-PSS electrode	0.30 V vs Ag/AgCl.	1–320 μM	0.3 μM	–	[49]
PEDOT$_{SDS}$–nanoAg–MDB electrode	−0.05 V vs Ag/AgCl	10–560 μM	0.1 μM	2 nA/μM	The present work

Abbreviations: poly(4-styrenesulfonate), PSS; Meldola Blue, MDB; ordered mesoporous carbon, OMC; Ref, references
Working solution: PBS solutions pH 6–7 except AuNPs electrode which is indicated in Table 1.

3.6. Amperometric response of NADH at PEDOT$_{SDS}$–nanoAg –MDB electrode

The optimization of applied potential for amperometric studies was performed at the PEDOT$_{SDS}$–nanoAg–MDB electrode for 10 μM NADH and was maximum current response observed at an applied potential of −0.05 V. Thus, the applied potential of −0.05 V was chosen for further amperometric study.

Fig. 7A shows the amperometric response of the PEDOT$_{SDS}$–nanoAg–MDB electrode for successive additions of NADH into stirring phosphate buffer solution. As seen from the first addition, clear and measurable current steps were apparent, and a linear relationship between the anodic current and NADH concentration was observed. At higher concentration values, a leveling-off was observed. The electrode response time was less than 7 s after addition of NADH until steady-state values were obtained. The fast response is attributed to an active film and short penetration depth of NADH. At higher concentration range the noise of the amperometric signal becomes larger as well as response current decreased, which can be attributed to the restrictions of NADH diffusion at this concentration range. Fig. 7B shows the calibration graph for NADH which spread in the range of 10–560 μM. The detection limit (S/N = 3), and sensitivity were found to 0.1 μM and 2 nA/μM, respectively. Table 1 gives the comparison of developed PEDOT$_{SDS}$–nanoAg–MDB electrode with other biosensors reported in the literature for the detection of NADH. The developed PEDOT$_{SDS}$–nanoAg–MDB electrode working potential and detection limit is comparable with literature reported in Table 1 [13,24,38,42–49].

Finally, we investigated the effect of interfering species commonly found in biological samples such as DA, UA and H$_2$O$_2$, as shown in Fig. 8. The addition of NADH results in a well-defined response, however, the successive addition of interfering species such as DA, and UA did not bring out discernible current response. On the other hand, H$_2$O$_2$ was found to produce very slight response current and it was negligible when compared with NADH current response. Though, the prepared modified electrode is good for NADH sensor, and worth comparable analytical data such as linear range, detection limit with literatures (Table 1), however, it had affected by ascorbic acid (AA). We are trying to minimize the interference of AA on our next part of the experiments.

The stability of modified electrode was also examined in the presence of NADH for 20 min under stirring condition by an amperometrically. The decrease of current was ~15% even in stirring condition. It indicates that modified electrode is stable and suitable for sensor applications.
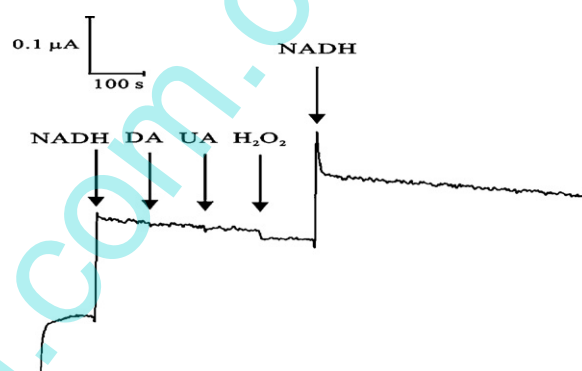

Fig. 8. Typical amperometric responses of NADH, UA, DA, and H$_2$O$_2$ at =−0.05 V under stirring condition.

4. Conclusions

PEDOT$_{SDS}$–nanoAg electrode was prepared by electrochemical deposition method. The nanoAg formation was confirmed by UV–vis spectroscopy and it shows SPR peak at around 375 nm. The PEDOT$_{SDS}$–nanoAg electrode has been employed as a platform to immobilize electrochemically active mediator, MDB. The PEDOT$_{SDS}$–nanoAg–MDB electrode exhibited electrocatalytic activity towards oxidation of NADH with 650 mV decrease over-potential. The modified electrode showed amperometric response with linear range 10–560 μM, detection limit 0.1 μM for NADH. Also, electrode showed diminished response from its interferences.

References

[1] P.N. Bartlett, E. Simon, C.S. Toh, Modified electrodes for NADH oxidation and dehydrogenase-based biosensors, Bioelectrochemistry 56 (2002) 117–122.
[2] J. Moiroux, P.J. Elving, Effect of adsorbtion, electrode material, operational variables on the oxidation dihydronicotinamide adenine dinucleotide at carbon electrodes, Anal. Chem. 50 (1978) 1056–1062.
[3] W.J. Blaedel, R.A. Jenkins, Electrochemical oxidation of reduced nicotinamide adenine dinucleotide, Anal. Chem. 47 (1975) 1337–1343.
[4] L. Gorton, E. Dominguez, Electrochemistry of NAD(P)$^+$/NAD(P)H, in: G.S. Wilson (Ed.), Encyclopedia of Electrochemistry (Bioelectrochemistry), vol. 9, Wiley–VCH, Weinheim, 2002, pp. 67–143.

[5] N. Mano, A. Kuhn, Immobilized nitro-fluorenone derivatives as electrocatalysts for NADH oxidation, J. Electroanal. Chem. 477 (1999) 79–88.

[6] C.R. Raj, B.K. Jena, Efficient electrocatalytic oxidation of NADH at gold nanoparticles self-assembled on three-dimensional sol–gel network, Chem. Commun. (2005) 2005–2007.

[7] B. Grundig, G. Wittstock, U. Rudel, B. Strehlitz, Mediator-modified electrodes for electrocatalytic oxidation of NADH, J. Electroanal. Chem. 395 (1995) 143–157.

[8] M. Ohatani, S. Kuwabata, H. Yoneyama, Electrochemical oxidation of reduced nicotinamide coenzymes at Au electrodes modified with phenothiazine derivative monolayers, J. Electroanal. Chem. 422 (1997) 45–54.

[9] M.I. Alvarez-Gonzalez, S.B. Saidman, M.J. Jesu's Lobo-Castanon, A.J. Miranda-Ordieres, P. Tunon-Blanco, Electrocatalytic detection of NADH and glycerol by NAD⁺-modified carbon electrodes, Anal. Chem. 72 (2000) 520–527.

[10] E. Katz, T. Lotzbeyer, D.D. Schlereth, W. Schuhmann, H.L. Schmidt, Electrocatalytic oxidation of reduced nicotinamide coenzymes at gold and platinum electrode surfaces modified with a monolayer of pyrroloquinoline quinone. Effect of Ca²⁺ cations, J. Electroanal. Chem. 373 (1994) 189–200.

[11] C.A. Pessoa, Y. Gushikem, L.T. Kubota, Ferrocenecarboxylic acid adsorbed on Nb₂O₅ film grafted on a SiO₂ surface: NADH oxidation study, Electrochim. Acta 46 (2001) 2499–2505.

[12] M. Musameh, J. Wang, A. Merkoci, Y. Lin, Low-potential stable NADH detection at carbon-nanotube-modified glassy carbon electrodes, Electrochem. Commun. 4 (2002) 743–746.

[13] S. Chakraborty, C. Retna Raj, Amperometric biosensing of glutamate using carbon nanotube based electrode, Electrochem. Commun. 9 (2007) 1323–1330.

[14] A. Salimi, R. Hallaj, M. Ghadermazi, Modification of carbon ceramic electrode prepared with sol–gel technique by a thin film of chlorogenic acid: application to amperometric detection of NADH, Talanta 65 (2005) 888–894.

[15] M. Huang, H. Jiang, J. Zhai, B. Liu, S. Dong, A simple route to incorporate redox mediator into carbon nanotubes/Nafion composite film and its application to determine NADH at low potential, Talanta 74 (2007) 132–139.

[16] P.de.S. Alvarez, P.R. Granda, M.J.L. Castanon, A.J.M. Ordieres, P.T. Blanco, New scheme for electrochemical detection of DNA based on electrocatalytic oxidation of NADH, Electrochem. Commun. 5 (2003) 267–271.

[17] B. Prieto-Simon, E. Fabregas, Comparative study of electron mediators used in the electrochemical oxidation of NADH, Biosens. Bioelectron. 19 (2004) 1131–1138.

[18] A. Curulli, F. Valentini, G. Padeletti, M. Viticoli, D. Caschera, G. Palleschi, Smart (Nano) materials: TiO₂ nanostructured films to modify electrodes for assembling of new electrochemical probes, Sens. Actuators B: Chem. 111 (2005) 441–449.

[19] J. Huang, D. Wang, H. Hou, T. You, Electrospun palladium nanoparticle-loaded carbon nanofibers and their electrocatalytic activities towards hydrogen peroxide and NADH, Adv. Funct. Mater. 18 (2008) 441–448.

[20] P.N. Bartlett, E. Simon, Poly(aniline)–poly(acrylate) composite films as modified electrodes for the oxidation of NADH, Phys. Chem. Chem. Phys. 2 (2000) 2599–2606.

[21] S.J. Tian, J.Y. Liu, T. Zhu, W. Knoll, Polyaniline doped with modified gold nanoparticles and its electrochemical properties in neutral aqueous solution, Chem. Commun. (2003) 2738–2739.

[22] S. Tian, J. Liu, T. Zhu, W. Knoll, Polyaniline/gold nanoparticle multilayer films: assembly, properties, and biological applications, Chem. Mater. 16 (2004) 4103–4108.

[23] R. Gangopadhyay, A. De, Conducting polymer nanocomposites: a brief overview, Chem. Mater. 12 (2000) 608–622.

[24] K.M. Manesh, P. Santhosh, A. Gopalan, K.P. Lee, Electrocatalytic oxidation of NADH at gold nanoparticles loaded poly(3,4-ethylenedioxythiophene)–poly(styrene sulfonic acid) film modified electrode and integration of alcohol dehydrogenase for alcohol sensing, Talanta 75 (2008) 1307–1314.

[25] B. Fan, X. Mei, J. Ouyang, Significant conductivity enhancement of conductive poly(3,4-ethylenedioxythiophene):poly(styrenesulfonate) films by adding anionic surfactants into polymer solution, Macromolecules 41 (2008) 5971–5973.

[26] N. Sakmeche, S. Aeiyach, J.J. Aaron, M. Jouini, J.C. Lacroix, P.C. Lacaze, Improvement of the electrosynthesis and physicochemical properties of poly(3,4-ethylenedioxythiophene) using a sodium dodecyl sulfate micellar aqueous medium, Langmuir 15 (1999) 2566–2574.

[27] A. Ramasubbu, A. Vanangamudi, S. Muthusubramanian, M.S. Ramachandran, S. Sivasubramanian, Electrocatalytic studies using silver–clay composite—a novel material, Electrochem. Commun. 2 (2000) 56–64.

[28] V.V. Vukovic, J.M. Nedeljkovic, Surface modification of nanometer-scale silver particles by imidazole, Langmuir 9 (1993) 980–983.

[29] V.S. Vasantha, S.M. Chen, Electrocatalysis and simultaneous detection of dopamine and ascorbic acid using poly(3,4-ethylenedioxy)thiophene film modified electrodes, J. Electroanal. Chem. 592 (2006) 77–87.

[30] C.M. Maroneze, L.T. Arenas, R.C.S. Luz, E.V. Benvenutti, R. Landers, Y. Gushikem, Meldola blue immobilized on a new SiO₂/TiO₂/graphite composite for electrocatalytic oxidation of NADH, Electrochim. Acta 53 (2008) 4167–4175.

[31] K.R. Brown, A.P. Fox, M.J. Natan, Morphology-dependent electrochemistry of cytochrome c at Au colloid-modified SnO₂ electrodes, J. Am. Chem. Soc. 118 (1996) 1154–1157.

[32] A. Henglein, Colloidal silver nanoparticles: photochemical preparation and interaction with O₂, CCl₄, and some metal ions, Chem. Mater. 10 (1998) 444–450.

[33] N.R. Jana, T.K. Sau, T. Pal, Growing small silver particle as redox catalyst, J. Phys. Chem. B 103 (1999) 115–121.

[34] A.M. Lazarin, C. Airoldi, Synthesis and electrochemical properties of meldola blue intercalated into barium and calcium phosphates, Sens. Actuators B 107 (2005) 446–453.

[35] A.C. Pereira, D.V. Macedo, A.S. Santos, L.T. Kubota, Amperometric biosensor for lactate based on Meldola's blue adsorbed on silica gel modified with niobium oxide, Electroanalysis 18 (2006) 1208–1214.

[36] A.J. Bard, L.R. Faulkner, Electrochemical Methods: Fundamentals and Applications, Wiley, New York, 1980.

[37] F.D. Munteanu, L.T. Kubota, L. Gorton, Effect of pH on the catalytic electrooxidation of NADH using different two-electron mediators immobilised on zirconium phosphate, J. Electroanal. Chem. 509 (2001) 2–10.

[38] L. Zhu, J. Zhai, R. Yang, C. Tian, L. Guo, Electrocatalytic oxidation of NADH with Meldola's blue functionalized carbon nanotubes electrodes, Biosens. Bioelectron. 22 (2007) 2768–2773.

[39] L. Mao, K. Yamamoto, Glucose and choline on-line biosensors based on electropolymerized Meldola's blue, Talanta 51 (2000) 187–195.

[40] N.S. Alvarez, P.M. Ortea, A.M. Paneda, M.J.L. Castanon, A.J.M. Ordieres, P.T. Blanco, A comparative study of different adenine derivatives for the electrocatalytic oxidation of β-nicotinamide adenine dinucleotide, J. Electroanal. Chem. 502 (2001) 109–117.

[41] V. Rosca, L. Muresan, I.C. Popescu, C. Cristea, A. Silberg, Gold electrodes modified with new phenothiazine derivative for electrocatalytic oxidation of NADH, Electrochem. Commun. 3 (2001) 439–445.

[42] T.N. Rao, I. Yagi, T. Miwa, D.A. Tryk, A. Fujishima, Electrochemical oxidation of NADH at highly boron-doped diamond electrodes, Anal. Chem. 71 (1999) 2506–2511.

[43] C.E. Banks, R.G. Compton, Exploring the electrocatalytic sites of carbon nanotubes for NADH detection: an edge plane pyrolytic graphite electrode study, Analyst 130 (2005) 1232–1239.

[44] L. Tang, G. Zeng, G. Shen, Yi. Zhang, Y. Li, C. Fan, C. Liu, C. Niu, Highly sensitive sensor for detection of NADH based on catalytic growth of Au nanoparticles on glassy carbon electrode, Anal. Bioanal. Chem. 393 (2009) 1677–1684.

[45] H.M. Nassef, A.E. Radi, C.K. O'Sullivan, Electrocatalytic sensing of NADH on a glassy carbon electrode modified with electrografted o-aminophenol film, Electrochem. Commun. 8 (2006) 1719–1725.

[46] S. Chakraborty, C. Retna Raj, Mediated electrocatalytic oxidation of bioanalytes and biosensing of glutamate using functionalized multiwall carbon nanotubes-biopolymer nanocomposite, J. Electroanal. Chem. 609 (2007) 155–162.

[47] L. Zhu, R. Yang, X. Jiang, D. Yang, Amperometric determination of NADH at a Nile blue/ordered mesoporous carbon composite electrode, Electrochem. Commun. 11 (2009) 530–533.

[48] H. Dai, H. Xu, Y. Lin, X. Wu, G. Chen, A highly performing electrochemical sensor for NADH based on graphite/poly(methylmethacrylate) composite electrode, Electrochem. Commun. 11 (2009) 343–346.

[49] M. Zhang, A. Yamaguchi, K. Morita, N. Teramae, Electrochemical synthesis of Au/polyaniline–poly(4-styrenesulfonate) hybrid nanoarray for sensitive biosensor design, Electrochem. Commun. 10 (2008) 1090–1093.